

Broadband Small-Signal Model and Parameter Extraction For deep sub-micron MOSFETs Valid up to 110 GHz

M. T. Yang, Patricia P. C. Ho, Y. J. Wang, T. J. Yeh, Y. T. Chia

Taiwan Semiconductor Manufacture Company, Ltd.
9, Creation Rd. I, Science-Based Industrial Park
Hsin-Chu, Taiwan, R.O.C.

Abstract — A broadband small-signal model suitable for deep sub-micron MOSFET high frequency applications and its parameter extraction have been proposed and demonstrated. Using a 110GHz millimeter wave S-Parameter measurement, we directly extracted the parameters and fitted very well within a broad range from 45MHz up to 110GHz. This is a state-of-the-art technique that demonstrates the model up to 110GHz and can be considered as an initial method for an optimization procedure to be used for more complete models.

considered as extraction routines for single-geometry transistor prior to extraction on the higher level of generating scalable model parameters.

This paper is organized as follows: Section II presents the small-signal equivalent circuit, section III describes the characterization of 110GHz mm_wave S-Parameters, section IV describes the extraction procedure, section V presents the validation of the extraction methodology, and section VI adds some concluding remarks.

I. INTRODUCTION

With the very high f_T of deep sub-micron MOSFETs of more than 100GHz, many high-speed or radio-frequency integrated circuits (RF ICs) which were fabricated exclusively in III-V or bipolar technologies are likely to be implemented in CMOS technology. This is because of its low cost, high level of integration and easy access to the technology [1,2]. This clearly opens the door to highly integrated full CMOS solutions for wireless applications. For circuit development, the construction of precise small-signal models and the extraction of their parameters are very important not only for device characterization but also for the circuit design. Several methods of extracting small-signal equivalent circuit parameters from the S-parameter measurement data have been reported [3]-[5]. However, these methods either require complex curve fitting and optimization steps, or do not account for the effect of the substrate resistance. This present work refers to the previous works of Sung et al. [6] and Kwon et al. [7], but provides improvement on some crucial points. To the author's knowledge, this work is the first to describe an accurate and systematic extraction technique, without requiring further fitting or tuning to precisely model the device performance from dc to millimeter-wave frequencies (mm_wave), including which including the substrate-related parameters and a complete set of non-quasi static (NQS) resistance. In addition, the fitting result targeted for the RF figure-of-merit (FOM) for f_T and f_{MAX} are also presented. Our result can be

II. SMALL-SIGNAL EQUIVALENT CIRCUIT

The proposed equivalent circuit suitable for high frequency applications used in this paper is based on the original SPICE equivalent circuit for the MOSFET [8]. Fig. 1 depicts the modified equivalent circuit with the added improvement under the substrate short-circuited to source condition. The new elements added to this equivalent circuit include R_{gs} , R_{gd} , R_{db} , C_{ds} , and L_g . The resistance R_{gs} represents the effective channel resistance seen by the signal flowing via C_{gs} from gate to source. It is an effective representation of the distributed resistance of the channel and of spreading bulk resistance capacitively coupled to the channel and is responsible for the real part of intrinsic Y_{11} . This element is important to input impedance matching in analog circuit designs. The resistance, R_{gd} , is analogous to R_{gs} but is associated with gate-to-drain capacitance. The bulk spreading resistance is represented by R_{db} . As the operational frequency increases, the impedance of the junction capacitance reduces. Thus, the substrate coupling effects through the drain junction and so substrate resistance becomes significant for the output impedance Y_{22} . The output capacitance, C_{ds} , resulting from capacitively coupling between fingered structures, is important for the output admittance Y_{22} in the mm_wave regime as the transistor dimension shrinks. Furthermore, an inductor, L_g , associated with the deep sub-micron poly gate is included to better fit the input admittance Y_{11} at mm_wave regime.

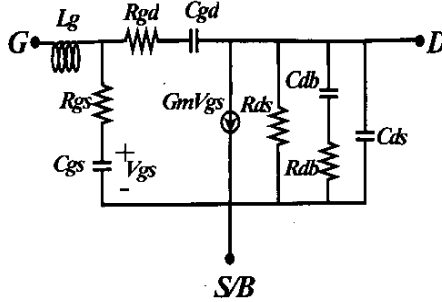


Fig. 1. Broadband small-signal equivalent circuit of the MOSFET used for mm-wave simulation.

III. MM_WAVE S-PARAMETER MEASUREMENT

The on-wafer mm-wave S-parameter measurement system consists of a Cascade wafer probe connected to an Agilent 8510XF Vector Network Analyzer (VNA). A self-consistent calibration technique performed using LRRM with Auto Load Inductance Compensation [9] was conducted to move the reference plane from the VNA output ports to the probe tips. A commercially available software package [10] was used for performing the calibrations. As a recommendation from Ref. [11], the thin Impedance Standard Substrate (ISS) included a layer of Radiation Absorption Material (RAM) between the ISS and metal chuck surface. After calibrating the VNA with impedance standard substrate, the S-parameters of the deep submicron RF NMOS transistor, fabricated using the TSMC 0.13 μ m process, were measured with the bulk tight to the source at different bias points ranging from 45MHz up to 110GHz. The device is configured with multi-fingered gate structure with a unit width of 2.5 μ m. In order to remove the pad parasitics, an accurate de-embedding technique was carried out. This was done by subtracting parasitics from both open and short structures. Once the transistors are de-embedded, the RF characteristics are then analyzed. Figure 2 shows the frequency response of current gain (H21) and power gain (MSG/MAG) at $V_d=1V$ and $V_g=0.7V$. The RF FOM such as f_T and f_{MAX} at various biases are then depicted in Fig. 3. A peak f_T of 130GHz and a peak f_{MAX} of 100GHz have been demonstrated. This clearly opens the door to highly integrated full CMOS solutions for wireless applications. The “best fit” result is also plotted in these figures for comparison. This is the first work that demonstrates a positive “best fit” both in the f_T and f_{MAX} up to 110 GHz and will be discussed in the next sections.

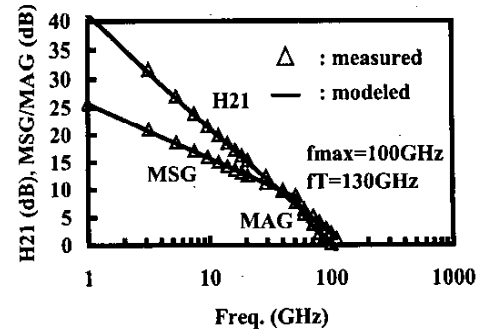


Fig. 2. Comparison between measured (marker) and modeled (line) current gain (H21) and power gain (MSG/MAG) frequency responses.

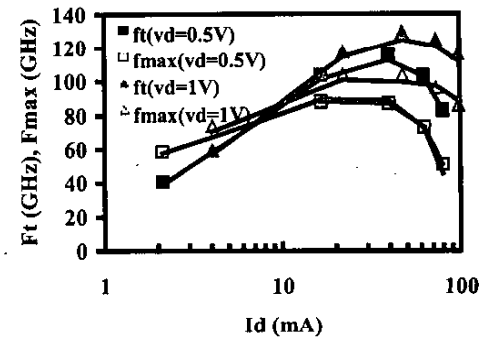


Fig. 3. Comparison between modeled (line) and measured (marker) f_T and f_{MAX} as a function of drain current at different V_d .

IV. PARAMETER EXTRACTION

By analyzing a Y-parameter on the equivalent circuit of the MOSFET for high-frequency operations, as discussed previously, direct extraction is performed. Each component of the equivalent circuit is extracted by using Y-parameter analysis and analytical equations are derived from both the real and imaginary parts of the Y-parameter. G_m is obtained from the $\text{Re}[Y_{21}-Y_{12}]$ and R_{ds} is extracted from the y-intercept of $1/\text{Re}[Y_{22}+Y_{12}]$ versus the frequency at the low frequency range. R_{gs} , R_{gd} , C_{gs} , and C_{gd} can be obtained as follows:

$$R_{gs} = \text{Re} \left\{ \frac{1}{Y_{11} + Y_{12}} \right\} \quad (1)$$

$$R_{gd} = -\operatorname{Re} \left\{ \frac{1}{Y_{12}} \right\} \quad (2)$$

$$C_{gs} = -\frac{1}{\omega} \frac{1}{\operatorname{Im} \left\{ \frac{1}{Y_{11} + Y_{12}} \right\}} \quad (3)$$

$$C_{gd} = \frac{1}{\omega} \frac{1}{\operatorname{Im} \left\{ \frac{1}{Y_{11}} \right\}} \quad (4)$$

For the extraction of substrate components, C_{db} , R_{db} , and C_{ds} are defined as follows:

$$C_{db} = -\frac{1}{\omega} \operatorname{Im} \left\{ Y_{22} + Y_{12} - \frac{1}{R_{ds}} \right\} \quad (5)$$

$$R_{db} = \operatorname{Re} \left\{ \frac{1}{Y_{11} + Y_{12}} \right\} - R_{ds} \quad (6)$$

$$C_{ds} = \frac{1}{\omega} \operatorname{Im} \left\{ Y_{22} + Y_{12} \right\}_{\omega \rightarrow \infty} - C_{db} \quad (7)$$

V. RESULT AND DISCUSSION

The salient feature of this work is to make use of a broadband measurement to facilitate the parameter determination by neglecting some of terms depending on the frequency range. In this approach, we started from the extraction of R_{ds} and G_m at low frequencies. After the extraction of R_{gs} and C_{gs} , the R_{gd} and C_{gd} are then determined. The admittances are determined at low frequencies and the impedances are determined at high frequencies. Continuing with the extraction of C_{db} and R_{db} at high frequencies, the routine is completed with the determination of the high frequency parasitics of C_{ds} and L_g . The C_{ds} is determined at the most extreme frequency. The L_g is identified based on a measurement simulation after all the parameters are determined by the "best fit" C_{gs} and C_{gd} and is 5.5pH for all biases. The proposed direct extraction method was applied to determine the parameters of the test device, which was multi-fingered n-MOSFET fabricated using TSMC 0.13μm technology with gate over ashed. Fig. 4 shows the frequency dependence of the extracted parameters and their values at $V_{ds}=1V$ and $V_{gs}=0.7V$. We selected a sub-range of the measured data, where the data represents a straight line. This allowed us to check whether the model is able to fit the measured data and enables us to easily extract the parameter as the mean value of that flat range. The average values of the extracted parameters at various

biases covering regions of saturation, sub-threshold, and linear are summarized in Table I. Calculated f_T as high as 120GHz can be obtained at $V_d=1V$ and $V_g=0.7V$, which closely matches the measurement. Both the NQS resistances of R_{gs} and R_{gd} are a function of the biasing conditions. This cannot be modeled by merely adding a single gate resistance similar to several CMOS RF models based on BSIM3v3 that have been proposed. In addition, there is also evidence that significant R_{db} cannot be neglected due to the existence of junction capacitance as compared with R_{ds} .

In Fig. 5, the simulation results for S-parameters obtained by using the equivalent circuit, shown in Fig. 1 with extracted values shown in Table I, is compared with the measured data at various biases. Excellent agreement in 4 S-parameters at low frequency for all biases indicates the proposed method is accurate and reliable for G_m , R_{ds} , R_{gs} , C_{gs} , R_{gd} , C_{gd} , and C_{db} , respectively. A sound prediction in the kink behavior of S_{22} at high frequency supports the extraction of R_{db} and C_{ds} . During the simulation, we observed that L_g is necessary for the prediction of the kink behavior in S_{11} at high frequency. The comparison between the extracted H_{21} and MSG/MAG from both measurement and simulation at $V_d=1V$ and $V_g=0.7V$ is plotted in Fig. 2. We also compared the f_T and f_{max} at various biases as shown in Fig. 3. Both results clearly indicate the validation of this model and proposed extraction method.

VI. CONCLUSION

A broadband small-signal model including the substrate-related parameters and a complete set of NQS resistance suitable for deep sub-micron MOSFET RF circuit development has been proposed. With a broadband S-parameter measurement from 45MHz up to 110GHz, the model parameters are directly extracted by using the frequency behavior of the device. An RF NMOS with an f_T of 130GHz and an f_{max} of 100GHz has been characterized and modeled. Excellent agreement in S-parameter values has been demonstrated. Well-matched results for the frequency response of H_{21} and MSG/MAG, and current response of f_T/f_{max} have also verified. Extraction results have been analyzed and discussed. Our method can be considered as an initial method for an optimization procedure to be used for more complete models.

REFERENCES

[1] Y. Taur et al. in *IEEE Electron Devices Meeting Tech. Dig.*, pp. 127-130, Dec. 1993.

[2] S. P. Voinigescu et al. in *IEEE Electron Devices Meeting Tech. Dig.*, pp. 721-724, Dec. 1995.

[3] G. Dambrine et al. in *IEEE Trans. Microwave Theory Tech.*, vol. 36, pp. 1151-1159, June 1988.

[4] S. Lee et al. in *IEEE Microwave Guided Wave Lett.*, vol. 7, pp. 75-77, March 1997.

[5] A. Pascht et al. in *IEEE Trans. Microwave Theory Tech.*, vol. 50, pp. 1503-1509, June 2002.

[6] R. Sung et al. in *IEEE Trans. Electron Devices*, vol. 45, pp. 1769-1775, Aug. 1998.

[7] I. Kwon et al. *IEEE Trans. Microwave Theory Tech.*, vol. 50, pp. 1503-1509, June 2002.

[8] L. W. Nagel, in Memo. ERL-M520, Univ. of California, Berkeley, 1975

[9] J. Pence, *42nd ARFTG Conference Dig.*, Nov. 1993.

[10] WinCal 3.1 Calibration and Measurement Tool, Commercial Product, *Cascade Microtech Inc.*

[11] E. Godshalk, *40th ARFTG Conference Dig.*, Dec. 1992.

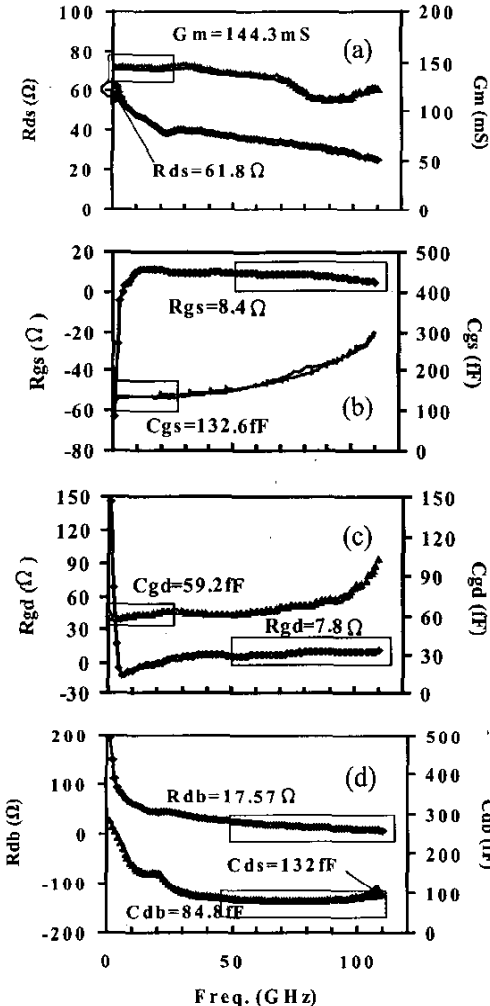


Fig. 4. Direct visual extraction for parameters of (a) R_{ds}/G_m , (b) R_{gs}/C_{gs} , (c) R_{gd}/C_{gd} , and (d) $R_{db}/C_{db}/C_{ds}$ at $V_d=1V$ and $V_g=0.7V$.

Table I. Parameter values extracted from measurements for device with various biases

	$V_d=1V; V_g=0.7V$	$V_d=0.5V; V_g=1.1V$	$V_d=0.5V; V_g=0.7$	$V_d=1.0V; V_g=0.3V$
L_g (pF)	5.5	5.5	5.5	5.5
R_{gs} (Ω)	8.4	6.38	8.72	10.2
C_{gs} (Ω)	132.6	109.6	133	126.9
R_{gd} (Ω)	7.8	9.8	6.18	3.57
C_{gd} (fF)	59.2	60.6	68.16	88.4
G_m (mS)	144.3	54.1	131	89
R_{ds} (Ω)	61.8	218.3	41.5	8.9
C_{db} (fF)	84.8	69.3	83.4	42.7
R_{db} (Ω)	17.6	9.48	14.8	10.1
C_{ds} (fF)	13.2	10.4	9.1	9.2

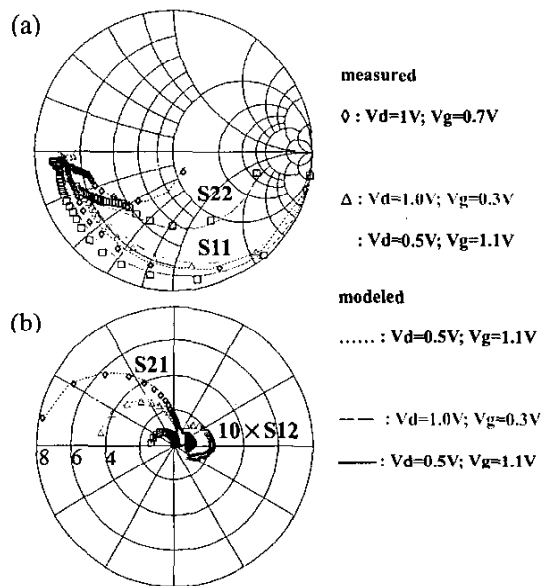


Fig. 5. Comparison between modeled and measured S-parameters, (a) Smith-chart, and (b) polar plot for device at different biases with frequency sweep from 45MHz ~110GHz.